High-pressure forms of lithium sulphate: Structural determination and computer simulation

David C. Parfitt,[1,*] David A. Keen,[1,2] Stephen Hull,[2] Wilson A. Crichton,[3] Mohamed Mezouar,[3] Mark Wilson,[4] and Paul A. Madden[5]

[1]*Department of Physics, Oxford University, Clarendon Laboratory, Parks Road, Oxford, OX1 3PU, United Kingdom*

[2]*The ISIS Facility, Rutherford Appleton Laboratory, Chilton, Didcot, Oxon OX11 0QX, United Kingdom*

[3]*European Synchrotron Radiation Facility, BP 220, F-38043 Grenoble, France*

[4]*Department of Chemistry, University College London, Christopher Ingold Laboratories, 20 Gordon Street, London WC1H 0AJ, United Kingdom*

[5]*Physical and Theoretical Chemistry Laboratory, Oxford University, South Parks Road, Oxford, OX1 3QZ, United Kingdom*

(Received 25 May 2005; revised manuscript received 29 June 2005; published 22 August 2005)

Powder x-ray diffraction has been performed on lithium sulphate, Li_2SO_4, in the temperature range 300 to 1000 K and at pressures up to 7.5 GPa. The ambient pressure β phase appears stable up to 3 GPa, whereupon a slow transformation begins into a new phase, δ-Li_2SO_4. This phase is characterized by broad, very low intensity Bragg peaks. Above 7 GPa and with slight heating, another phase, ϵ-Li_2SO_4, is formed which shows sharp Bragg peaks. Rietveld refinement of the structure of the ϵ phase has shown it to be isostructural to the high-temperature phase III of Na_2SO_4. Molecular dynamics simulations of the ϵ phase using an established potential indicate disordering of the lithium ions and rotations of the sulphate groups at high temperature, but not at a level approaching the extreme disordering shown in the superionic α form of Li_2SO_4.

DOI: 10.1103/PhysRevB.72.054121 PACS number(s): 61.10.Nz, 61.43.Bn, 61.50.Ks

I. INTRODUCTION

Under ambient conditions, lithium sulphate exists as a fully ordered monoclinic crystal, β-Li_2SO_4,[1–3] with a slightly distorted face-centered-cubic (fcc) arrangement of sulphate groups and lithium ions in the tetrahedral cavities. Above 846 K the crystal transforms into a superionic α phase, which shows extremely high values of ionic conductivity ($\sigma \simeq 1$–$3\ \Omega^{-1}\ cm^{-1}$).[4–6] Diffraction measurements[7–10] have confirmed the extensive disordering of the Li^+ ions, and also that the SO_4^{2-} units are orientationally disordered about their central sulfur atom. Structurally, α-Li_2SO_4 is related to the ambient temperature phase, though with a strict fcc array of sulphate groups. Detailed studies using single-crystal neutron diffraction[8,9] and diffuse scattering from powder neutron-diffraction data[10] have proposed similar models for the time-averaged structure of α-Li_2SO_4, though some controversy remains over the dynamic behavior. In particular, questions exist over the extent to which the conduction of the Li^+ ions and tumbling of the SO_4^{2-} groups are linked. These dynamic interactions have been modeled with some success using the potentials proposed in two molecular dynamics papers.[11,12] The simulations identify three separate contributions to the ionic conductivity: momentum transfer between rotating SO_4^{2-} units and the Li^+ ions (the "paddle-wheel" model); "gating" of Li^+ ion hops by a dynamic SO_4^{2-} sublattice; and simple percolation of Li^+ ions through a passive SO_4^{2-} sublattice.

Given the difficulty in both obtaining and interpreting experimental data on Li_2SO_4, it is perhaps understandable that its behavior under pressure has received little attention. Only one Raman spectroscopy study[13] has considered the topic in detail; two high-pressure phases are reported: the first (γ) exists between 1.3 and 3.5 GPa and the second (δ) is observed above 3.5 GPa. No quantitative structural details of the two high-pressure phases were provided.

This paper presents results from an x-ray diffraction study of powdered Li_2SO_4 to investigate its structural behavior at high pressure. The structures of the observed high-pressure phases are then used to provide some insight into the conduction mechanisms in Li_2SO_4.

II. EXPERIMENTAL METHOD

X-ray diffraction data were taken using the high-pressure beamline, ID30, at the European Synchrotron Radiation Facility in Grenoble, France. Li_2SO_4 powder of stated purity 99.99% from the Aldrich Chemical Company was finely ground and loaded into boron nitride (BN) containers. The container was surrounded by a graphite sheath and then by a boron-epoxy resin gasket. The outer diameter of the sample, BN container, and graphite sheath was approximately 1.0, 1.5, and 2.0 mm, respectively. The cell was heated by passing an electrical current through the graphite cylinder surrounding the inner BN container. The highly hygroscopic samples, once loaded in the pressure cell, were heated to $\simeq$500 K for 30 min to remove absorbed water. After this time, all peaks which were unambiguously attributed to the hydrated Li_2SO_4 phase in the diffraction patterns at ambient pressure had gone and it was believed that the sample only contained anhydrous Li_2SO_4 (but see Sec V). Further pressurization then took place at high temperature to seal the sample container fully.

During data collection the sample was illuminated with a 0.1×0.3 mm beam of monochromatic x rays with a wavelength of 0.158 16 or 0.533 966Å. Each data point was recorded using a Mar345 image plate for an exposure time of 120 s. The data obtained from the image plate were corrected for geometric distortions using the FIT2D program[14,15] and then integrated around the azimuthal angle to give one-dimensional diffraction data as a function of the scattering

angle, 2θ. The diffraction spectra were fitted using the GSAS Rietveld refinement program.[16]

The temperature of the sample was estimated using the power dissipated within the heating assembly, the power being calibrated using readings taken previously with a standard sample at a representative number of pressures and temperatures. Temperature gradients within the sample and calibration uncertainties resulted in errors of $\sim \pm 10$ K on the reported temperature.

The pressure exerted within the sample was calculated by *in situ* monitoring of the scattering from the boron nitride immediately surrounding the sample. These peaks were fitted again using the GSAS Rietveld refinement program, and the pressure extracted using the published equation of state of boron nitride.[17] Errors on the reported pressure due to calibration uncertainties were taken to be the larger of either 0.1 GPa or 10% of the absolute pressure.

III. EXPERIMENTAL RESULTS

Two experimental runs were made. The first pressurized a Li_2SO_4 sample at a constant temperature of 475 K to 7.5 GPa and then heated to 1000 K, at which point the sample containment failed. In the second run a sample was compressed rapidly, without collecting data, to 7 GPa at ~400 K; it was then cooled to room temperature and data were collected while the pressure was released in around 16 discrete steps. High temperatures were used to speed up the sluggish reaction kinetics,[13] and to reduce pressure-induced strain in the sample. (Preliminary measurements of the superionic α phase, formed above 848 K at ambient pressure, showed the rapid merging of the finely ground powder into a number of randomly orientated small crystallites. Data from this phase, which consisted of Debye-Scherrer rings with strongly modulated intensity and sharp Bragg spots, were not suitable for further analysis.)

At 475 K and above 3GPa the β-phase peaks began to lose intensity and a number of small extra peaks appeared (see Fig. 1). This is close to the position of a phase transition to the δ-Li_2SO_4 phase assigned by Lemos *et al.*[13] at 3.5 GPa. Of the peaks which appeared above 3 GPa, those that could be clearly identified were consistent with a hexagonal unit cell ($a=8.75$ Å, $c=7.02$ Å), with a volume ($V=465$ Å^3) which was $\sim 3/2\times$ the volume of β-Li_2SO_4. In addition to these "hexagonal" peaks, the diffraction spectra contained a large number of low-intensity broad peaks which could not be assigned to a single unit cell robustly.

Further application of pressure above 3 GPa led to a continued and significant loss of intensity in peaks from the monoclinic β phase, though this was not accompanied by a proportionate growth in the intensity of the hexagonal peaks. Overall, the peak intensities due to the β phase dropped by more than an order of magnitude between 2 and 7 GPa, though the β- and hexagonal phases were still both present at 7 GPa.

In both experimental runs the sample was slightly heated to ~500 K at 7 GPa in an attempt to sharpen the Bragg peaks. After this heating the ill-defined diffraction peaks faded and Bragg peaks from a new phase appeared. This

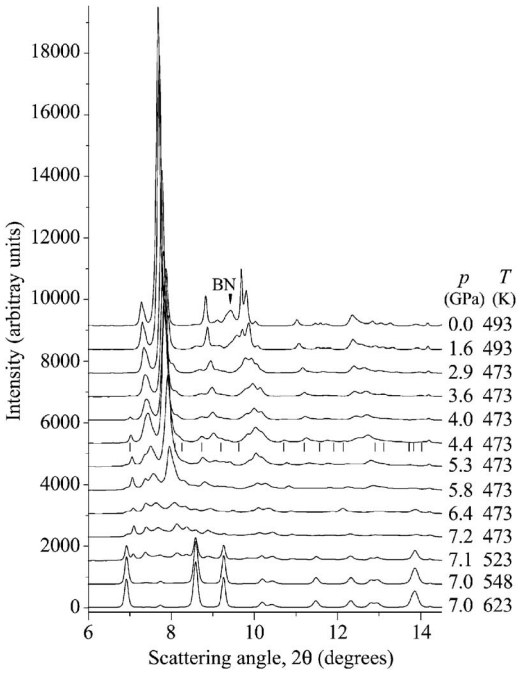

FIG. 1. A plot showing a selection of diffraction patterns over a reduced 2θ range from Li_2SO_4 at a number of different pressures on increasing pressure at ~500 K and on increasing temperature at ~7 GPa. "BN" marks the position of the main boron nitride reflection at ambient pressure and tick marks indicate the "hexagonal" peaks which appear in the intermediate pressure range. ($\lambda=0.533\,966$ Å for all patterns.)

phase, termed ϵ-Li_2SO_4, was stable up to the highest temperatures and pressures studied (7.5 GPa, 1000 K), though as with the α phase, higher temperatures increased the formation of small, single crystallites within the powdered sample.

During decompression the ϵ phase appeared relatively stable, with no sharp transition to any lower pressure phases. After release of pressure there was a slow reformation of the ambient pressure β phase, although this was not monitored to completion.

The high-pressure data for ϵ-Li_2SO_4 were indexed and fitted using an orthorhombic unit cell (space group *Cmcm*) and a structure similar to one of the high-temperature phases of sodium sulphate, Na_2SO_4-III.[18] The refined Na_2SO_4-III structure produced a reasonable fit to the ϵ-Li_2SO_4 data at 7.2 GPa and 723 K, with only a small mismatch of intensities in a subset of reflections. It was not possible to obtain a better fit by lowering the symmetry of the unit cell, for example to the *Pnma* structure of Na_2SO_4-II. Equally, further refinement of the atomic displacement parameters only produced a better fit with a highly anisotropic distribution for the sulphur ion, indicating large, unphysical one-dimensional displacements within its SO_4^{2-} cage. This anisotropic model was therefore disregarded. Instead, a simple preferred orientation correction, refining the second and fourth spherical harmonic preferred orientation terms, resulted in an acceptable fit, with $R_{wp}=8.5\%$. Details of the final refined parameters are presented in Table I and the fit is shown in Fig. 2. The volume of the ϵ phase is some 10% lower than that of the β phase at 7 GPa and 475 K, although this is subject to

TABLE I. Refined parameters for the high-pressure phase ϵ-Li_2SO_4 at 7.2 GPa and 723 K.

Space group	*Cmcm*
a,b,c	5.3452(2), 7.9323(3), 6.0292(3) Å
Formula units/unit cell	$Z=4$
Unit cell volume	255.64(2) Å^3
Li^+ 4(b)$(0,\frac{1}{2},0)$	$B_{Li1}=16.3(7)$ Å^2
Li^+ 4(c)$(0,y_{Li2},\frac{1}{4})$	$y_{Li2}=0.195(2)$
	$B_{Li2}=12.23(5)$ Å^2
S^{6+} 4(c)$(0,y_S,\frac{1}{4})$	$y_S=0.8570(2)$
	$B_S=3.20(4)$ Å^2
O^{2-} 8(f)$(0,y_{O1},z_{O1})$	$y_{O1}=0.2460(3)$; $z_{O1}=0.5575(4)$
	$B_{O1}=3.15(8)$ Å^2
O^{2-} 8(g)$(x_{O2},y_{O2},\frac{1}{4})$	$x_{O2}=0.2744(4)$; $y_{O2}=0.4610(3)$
	$B_{O2}=2.66(6)$ Å^2
Fit details	$N_{data}=2062$, $N_{obs}=182$,
	$N_v=31$, $R_p=0.0648$,
	$R_{wp}=0.0849$, $R_{exp}=0.0400$

some uncertainty owing to the difficulty in indexing the β phase at this pressure and the small increase in temperature required to form the ϵ phase.

The structure of ϵ-Li_2SO_4 (shown in Fig. 3) consists of an ordered arrangement of layers of isolated SO_4^{2-} units, each with an O1–O1 and O2–O2 bond aligned parallel to the c axis and a axis, respectively. Alternating layers perpendicular to c (at $z=0.25$ and $z=0.75$) possess SO_4^{2-} units aligned in opposite directions. The SO_4^{2-} tetrahedra are relatively undistorted, with two S–O bonds of length 1.419 Å and two of length 1.461 Å, and intratetrahedral bond angles of 109.75°, 111.24°, and four angles of 108.96°. The Li^+ ions sit in two positions within the SO_4^{2-} sublattice. The Li1 ion is surrounded by six O^{2-} ions at similar distances (two O1-type at 2.045° and four O2-type at 2.126°), each from a different neighboring SO_4^{2-} group. This produces an octahedral environment for the Li1 ion, with four O–Li1–O bond angles of 88.66° and 91.34° and two of 87.25° and 92.75°. In contrast, Li2 has four close O^{2-} neighbors (two O1-type at 1.897 Å and two O2-type at 2.214 Å), with two O2-type further away at 2.569 Å. This is a highly distorted environment. The two closest Li2-O distances at 1.897 Å and two furthest away at 2.569 Å are to O^{2-} ions from four distinct SO_4^{2-} groups, whereas the two Li2-O distances at 2.214 Å are to O^{2-} ions from the same SO_4^{2-} tetrahedron. The latter results in a relatively acute O–Li2–O bond angle of 66°.

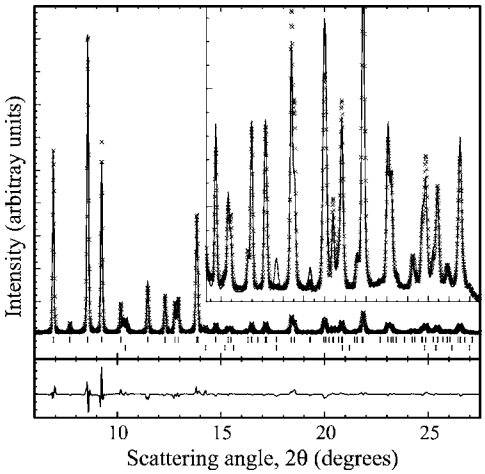

FIG. 2. Diffraction data ($\lambda=0.533\,966$ Å) from the ϵ phase of Li_2SO_4 at 7.2 GPa and 723 K (crosses) together with the calculated Rietveld fit (solid line). The difference between observed and calculated intensities is plotted at the bottom (on the same intensity scale as the main plot). Tick marks below the data indicate Bragg peak positions for ϵ-Li_2SO_4 (upper row) and hexagonal boron nitride (lower row). The intensity magnification in the inset is by a factor of 18.

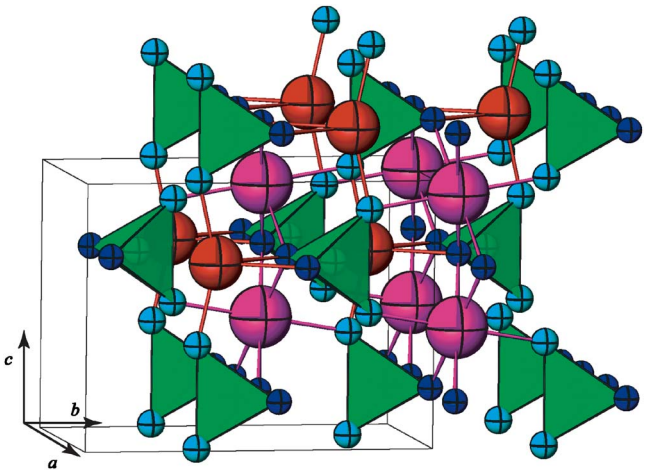

FIG. 3. (Color online) The structure of ϵ-Li_2SO_4 determined from x-ray diffraction data at 7.2 GPa and 723 K. SO_4^{2-} units are plotted as green tetrahedra, Li^+ ions are denoted by large pink (Li1, 4b) and large red (Li2, 4c) spheres; O^{2-} ions by small light blue (O1, 8f) and small dark blue (O2, 8g) spheres. Bonds connect Li^+ ions to their nearest oxygen neighbors.

IV. MOLECULAR DYNAMICS SIMULATIONS

There has already been some success in using molecular dynamics (MD) simulations to model the structure and dynamics of the α- and β phases of Li_2SO_4.[11,12] The simulations carried out here follow a similar method using fully ionic nonpolarizable SO_4^{2-} and Li^+ ions. We adopt without change many of the parameters used in the model of Klein *et al.*[12] However, instead of constraining the lengths of the S–O and O–O bonds within each sulphate group, we allow them to vary within a harmonic potential, with spring constants and equilibrium lengths determined from the vibrational spectra of Li_2SO_4.[19–21] The remaining intermolecular interactions are described by a standard potential, v, of the form

$$v_{\alpha,\beta}(r) = A_{\alpha,\beta}\exp(-a_{\alpha,\beta}r) + \frac{q_\alpha q_\beta e^2}{4\pi\epsilon_0 r}, \qquad (1)$$

where α and β label the ions, r is their separation, $q_\alpha e$ is the charge on ion α, $A_{\alpha,\beta}$ and $a_{\alpha,\beta}$ are an energy and inverse

TABLE II. Numerical values of the parameters used in the molecular dynamics simulations. Other interactions were vanishingly small and were neglected.

Exponential terms		
$\alpha-\beta$	$A_{\alpha\beta}$(MJ mol^{-1})	$a_{\alpha\beta}$(Å^{-1})
O—O	234.0	4.180
O—Li	16.5	3.255
Harmonic terms		
α-β	$k_{\alpha\beta}$(MJ mol^{-1} Å^{-2})	$R_{\alpha\beta}$(Å)
S—O	1.278	1.51
O—O	1.062	2.46

length for the interaction between ion α and ion β, respectively. As in previous work, the lithium ions are assigned a charge of e, whereas to model the covalent nature of the S–O bond the oxygen ions are assigned a charge of $-0.8e$ and the sulphur ions have the remaining $1.2e$. Numeric values for the remaining parameters are given in Table II. Simulations of the phases of Li_2SO_4 with known structures were carried out using these parameters, and stable structures of the ambient pressure α- and β-Li_2SO_4 phases with densities in good agreement with experiment were obtained. Furthermore, the β-Li_2SO_4 structure was stable to high pressures, presumably because the MD technique is not always amenable to studies of phase transitions and works most effectively for detailed studies of known phases.

The initial configurations for the simulations were based on the structure of ϵ-Li_2SO_4 determined from the analysis of the x-ray diffraction data as presented in Table I. The infinite crystal was constructed by applying periodic boundary conditions to a $3\times3\times3$ supercell, giving a total of 756 independent ions. The time step for force integration was 15 atomic units, or approximately 0.36 femtoseconds. Short simulations at constant temperature and pressure were carried out at a number of pressures up to 10 GPa and at temperatures up to the simulated melting point at each pressure. Each new simulation started with the atomic positions and simulation box size taken from the end of a previous simulation at similar pressure and temperature. Longer simulations (up to 10^6 time steps) were carried out at the higher temperatures to ensure that the simulated structures under these conditions were stable against the melting of the sulphate sublattice on a reasonable simulation time scale and to investigate diffusion processes.

The average ion positions from an MD simulation at 6.7 GPa and 700 K are given in Table III. These are in good agreement with those measured experimentally (see Table I) and show that the structure of ϵ-Li_2SO_4 is reproduced well by the MD simulation. The MD simulations also confirmed that the internal structural parameters do not change significantly with temperature within the ϵ phase.

Table IV shows the compressibility and expansivity of the high-pressure ϵ phase as calculated by fitting a second-order Birch-Murnaghan (i.e., $k'_0=4$) equation of state[22] to the experimental unit cell volume, determined over a limited range of pressures and temperatures, and assuming the thermal expansivity, $\alpha(T)=\alpha_0$. Parameters from the MD simulations are also given, obtained in the same way, but from data covering a more extensive range of pressure and temperature. The experimental and simulated parameters are in good agreement, further validating the potentials used in the simulations.

TABLE III. Average structural parameters for the high-pressure phase ϵ-Li_2SO_4 from an MD simulation at 6.7 GPa and 700 K.

Space group	*Cmcm*
a,b,c	5.24(4), 8.09(8), 5.89(4) Å
Formula units/unit cell	$Z=4$
Unit cell volume	250(6) Å^3
$Li1^+$ $4(b)\left(0,\frac{1}{2},0\right)$	(−0.0003[1], 0.5050[1], 0.0000[1])
$Li2^+$ $4(c)\left(0,y_{Li2},\frac{1}{4}\right)$	(−0.0001[3], 0.1961[6], 0.2500[2])
S^+ $4(c)\left(0,y_S,\frac{1}{4}\right)$	(0.0000[4], 0.8550[1], 0.2500[1])
$O1^{2-}$ $8(f)(0,y_{O1},z_{O1})$	(−0.010[9], 0.2450[1], 0.541[1])
$O2^{2-}$ $8(g)\left(x_{O2},y_{O2},\frac{1}{4}\right)$	(0.272[14], 0.4650[1], 0.250[1])

V. DISCUSSION

A. Structural changes in Li_2SO_4 at high pressure

There are some discrepancies between the phase behavior observed here and that reported previously based on Raman studies.[13] In particular, there is no evidence for the proposed $\beta\rightarrow\gamma$ transition at 1.3 GPa although, given the rather low symmetry and high degree of peak overlap in the β phase, our data do not preclude a subtle distortion of the LiO_6 octahedra as suggested by Lemos *et al.*[13] However, MD simulations of β-Li_2SO_4 also did not show any changes in the local environment of the Li^+ ion with increased pressure.

Based upon the $\gamma\rightarrow\delta$ transition pressure reported by Lemos *et al.*,[13] we have associated the sluggish transition which begins in our work around 3 GPa with the appearance of the δ phase. This phase produced broad, weak Bragg peaks, which may be the result of strain broadening, the incomplete formation of a single phase, or a very low symmetry structure. It is also possible that there is no thermodynamically stable intermediate phase, and the observed spectra are the result of a kinetically hindered transition to the higher pressure ϵ phase.

TABLE IV. Equation of state details for ϵ-Li_2SO_4 as derived from molecular dynamics simulations and compared with the values obtained from the diffraction data. V_0 refers to the unit cell volume at ambient pressure and 273 K.

	Simulation	Experiment
V_0(Å^3)	258.2(3)	277.2(6)
k_0(GPa^{-1})	48.9(8)	54(2)
k'_0 (Fixed)	4	4
$\alpha_0(\times10^{-5}$ K$^{-1})$	10.1(4)	8(2)
α_1 (Fixed) (K^{-2})	0	0
$\left(\frac{dk}{dT}\right)_p$	−0.014(1)	−0.015(8)

It is difficult to reconcile the hexagonal peaks and the large number of broad peaks which appear above 3 GPa with a single phase. It is possible that the hexagonal peaks correspond to a high-pressure modification of residual hydrated Li_2SO_4, occurring at levels which could not be detected at ambient pressure, given the similarities of the x-ray spectra of Li_2SO_4 and hydrated Li_2SO_4 at room temperature and pressure.[23–25] The lack of intensity increase of the hexagonal peaks as the β-phase peak intensities decrease and the existence of a transition in the hydrated compound at ~2.6 GPa (Ref. 25) support this possibility.

In the wider context of the family of sulphate-containing compounds, there has been the observation[25–30] that some lithium sulphate-based tertiary compounds (of the form $LiMSO_4$; M=Cs, K, Na, NH_4) exhibit a degree of orientational disordering of the SO_4^{2-} units upon pressurizing. There have also been claims of the formation of incommensurate structures and pressure-induced amorphization in $LiKSO_4$.[26–29] No increase in the level of diffuse scattering is observed in this high-pressure phase of Li_2SO_4, nor is any pressure-dependent qualitative change reported in the Raman spectra of Li_2SO_4,[13] both of which support the conclusion that disorder is not responsible for the poor resolution of the Bragg peaks observed in the δ phase. Sakuntala *et al.*[25] have proposed an overarching mechanism in which pressure-driven disordering in $LiMSO_4$ compounds is critically dependent on the degree of size mismatch between the Li^+ ion and the M^+ ion; a lack of disorder upon applied pressure in Li_2SO_4 is consistent with this scheme.

As noted previously, the high-pressure ϵ phase of Li_2SO_4 shares a structure with the high-temperature phase III of Na_2SO_4. The structure is part of a subgroup of the metathenardite stru cture ($P6_3/mmc$) with the group-subgroup transformation achieved by long-range ordering of the SO_4^{2-} units' orientation. Similar relationships have been shown to produce as many as 25 different structures based on the ordering of SO_4^{2-} units within sulphate compounds.[31]

B. Disorder in Li_2SO_4 at high pressures and temperatures

Much of the previous interest in Li_2SO_4 stems from the thermally induced disorder observed in the superionic α phase. It is therefore interesting to ascertain whether the high-pressure ϵ phase, with a structure entirely different from those of the α- and β phases, will also exhibit either sulphate group orientational disorder or lithium ion diffusion at high temperature. The results from the diffraction measurements taken at high temperature within the ϵ phase do not show extensive disorder. However, the data are unlikely to be sensitive to low levels of disorder, given the problems of obtaining good powders from Li_2SO_4 under high temperature and pressure conditions. Instead, and encouraged by the fact that the MD models of the ϵ phase produced good representative average structures at all temperatures, thermally induced disorder within ϵ-Li_2SO_4 was investigated further using MD simulation.

At ambient pressures, raising the temperature of the simulation of ϵ-Li_2SO_4 produces melting of the sulphate sublattice without the presence of an intermediate disordered phase. Some lithium ion diffusion and reorientation of SO_4^{2-} groups was observed, but only in simulations that were prone to melting as the simulations progressed. Simulations that did not melt displayed vanishingly small levels of disorder. At higher pressures ($\gtrsim$5 GPa) it was possible to stabilize configurations which exhibited low levels of orientational disorder in addition to the slow formation of lithium defects. The observed disorder was limited and existed, in a computationally sensible time scale, only for a narrow temperature range ($\simeq$50 K) just below the melting point.

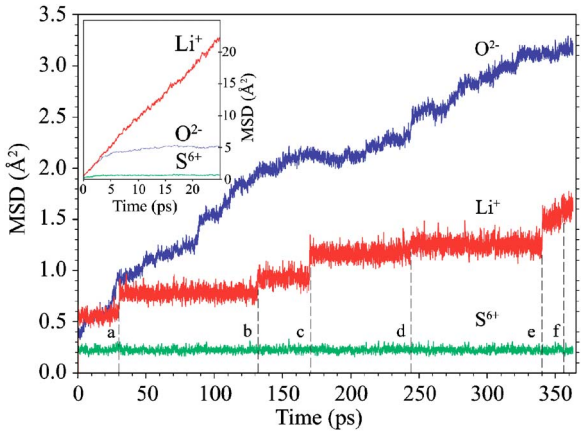

FIG. 4. (Color online) Mean-squared displacement of the S^{6+}, O^{2-}, and Li^+ ions within ϵ-Li_2SO_4 during the course of a single MD simulation simulation at 6.7 GPa and 1380 K. For comparison, the inset shows equivalent mean-squared displacements from MD simulations of the superionic α phase at 0.5 GPa and 800 K. Labels (a) to (f) identify Li^+ diffusive events.

Figure 4 shows the mean-squared displacements (msd) of the three constituent ions in ϵ-Li_2SO_4 from a very long (>350 ps) MD simulation at 7.2 GPa and a temperature that is $\simeq$10 K below the simulation melting temperature. It is evident that any ionic motion is very limited; the O^{2-} ion msd has not attained the "saturation" value expected for fully rotating SO_4^{2-} tetrahedra (reached in ~10 ps in the α phase—see the inset to Fig. 4), and the Li^+ ion msd shows several plateaus linked by a small number of jumps over a few time steps. These jumps are associated with very limited Li^+ migration through the sulphate ion lattice. Importantly, the jumps in the Li^+ msd are not coincident with substantial changes in the O^{2-} msd, indicating that they are not directly linked to SO_4^{2-} rotations.

To probe the dynamics in more detail, maps of the ion trajectories from the MD simulation at 7.2 GPa and 1380 K were constructed. Those Li^+ ions observed to diffuse are shown in Fig. 5. It is clear that the diffusion is only short range; a small number ($\leqslant$4) of neighboring Li^+ ions form correlated closed loops within the structure. The correlated nature of the diffusion explains why the jumps in Li^+ msd are sharp. Of the diffusive events clearly observed in the 350-ps-long MD simulation (see Fig. 4), the majority involved Li^+ ions moving from 4(c)→4(b) sites (and vice versa), some moving directly between 4(b) sites.

The O^{2-} trajectories from individual SO_4^{2-} groups show significant librational motion with occasional larger rotations of ~120° about a specific S–O bond. This shows that the

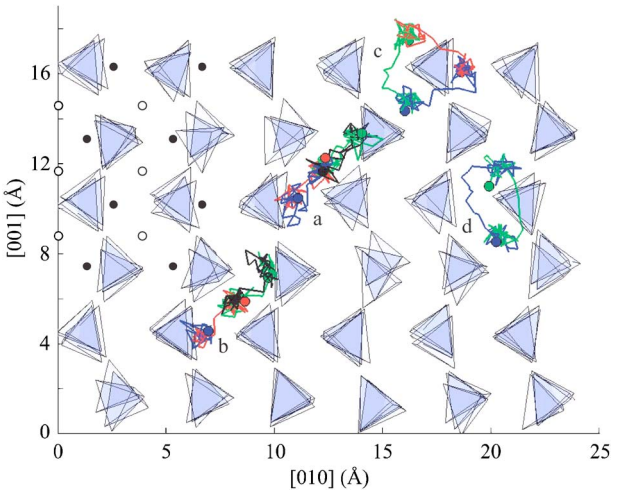

FIG. 5. (Color online) Plot of the $3\times3\times3$ MD configuration of ϵ-Li_2SO_4 at 7.2 GPa and 1380 K and projected down the [100] axis. The plot shows the instantaneous positions of the SO_4^{2-} groups at one time step together with the trajectories of the small number of Li^+ ions involved in local diffusion for 6000 time steps around the jumps in Li^+ ion msd. For clarity, the trajectories correspond to joining ion positions 100 time steps apart. The labels on the plot refer to specific jumps in Li^+ msd similarly identified in Fig. 4 and the colors to different Li^+ ions. The open and filled circles in the top left-hand corner indicate the positions of the octahedral 4(*b*) and distorted "tetrahedral" 4(*c*) positions, respectively.

SO_4^{2-} units are able to reorientate to each of their four equivalent symmetry positions, although free rotations appear sterically forbidden. This is in contrast to the behavior of the α phase, where a structural model with overall spherically symmetric O^{2-} density for the SO_4^{2-} groups best describes the diffraction data[8] and MD simulations show that the rate of SO_4^{2-} group reorientation is very rapid.[11]

VI. CONCLUSIONS

The structural behavior of Li_2SO_4 fits broadly within the general relationships observed in other related compounds. In the ambient pressure β phase the Li^+ ions occupy tetrahedral positions and, as shown in both experiment[8–10] and simulation,[12] the octahedral voids are too large to allow significant Li^+ ion occupancy. The rotation of the SO_4^{2-} units within the α phase also shows that inter-SO_4^{2-} group O—O interactions are not significant in determining the crystal structure. As the pressure is raised an octahedral coordination of the Li^+ becomes more favorable and also intersulphate group O—O interactions become more important as they become closer together.

In the α phase of Li_2SO_4 high levels of ionic conduction are observed, along with the rotation of the sulphate groups. In contrast, the disordering observed in MD simulations of the ϵ phase is on a far more modest scale, with a different packing of sulphate groups and no suitable vacant sites which can support the defect formation necessary for bulk cation migration. In some senses, the behavior of the ϵ phase of Li_2SO_4 may be compared with the high-temperature superionic cubic γ phase of Na_3PO_4, where sodium ions occupy all available octahedral and tetrahedral sites.[32,33] In this phase, although both octahedral and tetrahedral sites are involved in Na^+ ion conduction, neutron diffraction[32] and MD simulations[33] suggest that the Na^+ ions in octahedral sites are more readily mobile. Significant Na^+ diffusion is only observed in the MD simulations at temperatures above $\simeq$1200 K within superionic γ-Na_3PO_4, whereas the simulated transition to the γ phase is at $T_c\simeq620$ K. Furthermore, this diffusion is not correlated to PO_4-group rotations since they freely rotate at all temperatures above T_c.[33]

*Electronic address: d.c.parfitt@rl.ac.uk

[1] J. G. Albright, Z. Kristallogr. **84**, 150 (1932).
[2] N. W. Alcock, D. A. Evans, and H. D. B. Jenkins, Acta Crystallogr., Sect. B: Struct. Crystallogr. Cryst. Chem. **B29**, 360 (1973).
[3] A. Nord, Acta Crystallogr., Sect. B: Struct. Crystallogr. Cryst. Chem. **B32**, 982 (1976).
[4] B.-E. Mellander and D. Lazarus, Phys. Rev. B **31**, 6801 (1985).
[5] R. Tärneberg and A. Lundén, Solid State Ionics **90**, 209 (1996).
[6] B. M. Suleiman, M. Gustavsson, E. Karawacki, and A. Lundén, J. Phys. D **30**, 2553 (1997).
[7] T. Forland and J. Krogh-Moe, Acta Chem. Scand. (1947-1973) **11**, 565 (1957).
[8] L. Nilsson, J. O. Thomas, and B. C. Tofield, J. Phys. C **13**, 6441 (1980).
[9] R. Kaber, L. Nilsson, N. H. Andersen, A. Lundėn, and J. O. Thomas, J. Phys.: Condens. Matter **4**, 1925 (1992).
[10] L. Karlsson and R. L. McGreevy, Solid State Ionics **76**, 301 (1995).
[11] R. W. Impey, M. L. Klein, and I. R. McDonald, J. Chem. Phys. **82**, 4690 (1985).
[12] M. Ferrario, M. L. Klein, and I. R. McDonald, Mol. Phys. **86**, 923 (1995).
[13] V. Lemos, C. S. Sérgio, E. Cazzanelli, and A. Fontana, Phys. Rev. B **41**, 11593 (1990).
[14] A. P. Hammersley, S. O. Svensson, M. Hanfland, A. N. Fitch, and D. Häusermann, High Press. Res. **14**, 235 (1996).
[15] A. P. Hammersley, Tech. Report ESRF98HA01T, ESRF (1998).
[16] A. C. Larson and R. B. Von Dreele, Los Alamos National Laboratory Report LAUR 86-748 (1994).
[17] Y. L. Godec, D. Martinez-Garcia, M. Mezouar, G. Syfosse, J. P. Itie, and J. M. Besson, High Press. Res. **17**, 35 (2000).
[18] S. E. Rasmussen, J.-E. Jørgensen, and B. Lundtoft, J. Appl. Crystallogr. **29**, 42 (1996).
[19] R. Frech and E. Cazzanelli, Solid State Ionics **9-10**, 95 (1983).
[20] L. Börjesson and L. M. Torell, Phys. Rev. B **32**, 2471 (1985).
[21] L. Börjesson and L. M. Torell, Solid State Ionics **18-19**, 582 (1986).

[22] R. J. Angel, Rev. Mineral. Geochem. **41**, 35 (2001).
[23] J.-O. Lundgren, Å. Kvick, R. Karppinen, R. Liminga, and S. C. Abrahams, J. Chem. Phys. **80**, 423 (1984).
[24] R. Karppinen, R. Liminga, J.-O. Lundgren, Å. Kvick, and S. C. Abrahams, J. Chem. Phys. **85**, 5221 (1986).
[25] T. Sakuntala and A. K. Arora, Physica B **279**, 282 (2000).
[26] F. E. A. Melo, V. Lemos, F. Cerdeira, and J. Mendes Filho, Phys. Rev. B **35**, 3633 (1987).
[27] H. Sankaran, S. K. Sikka, S. M. Sharma, and R. Chidambaram, Phys. Rev. B **38**, 170 (1988).
[28] V. Lemos, R. Centoducatte, F. E. A. Melo, J. Mendes Filho, J. E. Moreira, and A. R. M. Martins, Phys. Rev. B **37**, 2262 (1988).
[29] A. K. Arora and T. Sakuntala, J. Phys.: Condens. Matter **4**, 8697 (1992).
[30] E. S. Silveira, P. T. C. Freire, O. Pilla, and V. Lemos, Phys. Rev. B **51**, 593 (1995).
[31] M. Kurzyński and M. Halawa, Phys. Rev. B **34**, 4846 (1986).
[32] R. J. Harrison, A. Putnis, and W. Kocklemann, Phys. Chem. Chem. Phys. **4**, 3252 (2002).
[33] W. G. Yin, J. J. Liu, C. G. Duan, W. N. Mei, R. W. Smith, and J. R. Hardy, Phys. Rev. B **70**, 064302 (2004).